On-line Monitoring of Methyl Methacrylate–Vinyl Acetate Emulsion Copolymerization

A. M. SANTOS,[1] G. FÉVOTTE,[2] N. OTHMAN,[3] S. OTHMAN,[2] T. F. MCKENNA[3]

[1] FAENQUIL, Rodovia Itajuba-Lorena, km 74.5, 12600000 Lorena/SP, Brazil

[2] L.A.G.E.P.-Université de Lyon I, and [3] C.N.R.S.—L.C.P.P./CPE 43 Blvd. du 11 Nov. 1918, 69622 Villeurbanne CEDEX, France

ABSTRACT: An adaptive calorimetric method, coupled with state estimators for emulsion copolymerization, is shown to provide accurate, on-line information on the evolution of the composition and kinetics of an emulsion copolymerization. This method was evaluated for the emulsion copolymerization of methyl methacrylate–vinyl acetate (MMA–VAc) under nonisothermal conditions. In addition to providing on-line estimates of the number of moles of each polymerizing species in the reactor, the state estimator provides a value for a lumped kinetic parameter proportional to the product of $\bar{n}N_p$. This information can be combined with off-line measurements to study the evolution of polymerization kinetics and to explain the trends observed for the molecular weight distribution and glass transition temperatures. Values of $\bar{n}$ were found to vary from 0.5 to 30 for the homopolymerization of MMA. However, the presence of VAc in the copolymerizing system drastically reduces $\bar{n}$. This can lead to a dramatic increase in the average molecular weight of the copolymer since it alters the ratio of propagation to termination in the polymerizing particles. © 2000 John Wiley & Sons, Inc. J Appl Polym Sci 75: 1667–1683, 2000

Key words: emulsion copolymerization; methyl methacrylate; vinyl acetate; kinetics; calorimetry

INTRODUCTION

To be able to follow the advancement of a polymerization reaction and to improve the quality of the control of polymer properties (such as copolymer composition and glass transition temperatures, which are often very difficult to measure in real time), it is important to define control strategies that exploit the relationships between the polymer microstructure, polymer "quality," and process conditions. Before one can do this, it is necessary to possess a means for the interpretation of on-line data (i.e., on-line sensors such as calorimetry plus state estimators) and that can help one follow key physical quantities such as the individual monomer conversions and polymer composition. The accurate kinetic data thus obtained can be used to develop and refine mechanistic models of the polymerization in question, as well as to contribute toward a better understanding of the polymeric microstructure and physical properties of the final material, such as the glass transition temperature.

ON-LINE ENERGY BALANCES: THE USE OF CALORIMETRY IN REACTOR MONITORING

One such method for the evaluation of polymerization kinetics is calorimetry, which is essen-

---

tially a quantification of the energy balance around the reactor:

$$m_r c_{p_r} \frac{\partial T_R}{\partial t} = Q_R - Q_j - Q_{\text{loss}} = \sum_{i=1}^{n} (R_{p_i}(-\Delta Hp_i))$$
$$- UA(T_R - T_j) - Q_{\text{loss}} \quad (1)$$

m_r is the mass of the reactor contents (plus agitator, etc.) and c_{p_r} is the summated average heat capacity of the reactor. Q_R (the heat of reaction) is a function of the individual polymerization rates, R_{p_i}, which are ultimately functions of individual monomer concentrations (and of the intrinsic value of the polymerization rate constants). The rate of heat removal through the jacket depends on UA, which is the product of the overall heat-transfer coefficient and the heat-transfer surface area; T_R, the reactor temperature; and T_j, the temperature of the cooling jacket. Q_{loss} is a heat-loss term that in this representation includes all energy loss to the environment, heat losses through a condenser, etc. To estimate $Q_R(t)$, we must use the other terms of Eq. (1) which must be measured or estimated.

Efforts using calorimetry to follow the reaction have been widely discussed in the literature for several years, and, therefore, we will not go into detail on this subject in the current work. It has been demonstrated by a number of other research groups that calorimetry provides us with a very useful on-line tool to understand what is happening during polymerization.[1–4] However, one of the biggest problems with the majority of the works dedicated to this form of application has been the fact that they employ lab-scale calorimeters that imply that the use of a number of technological choices be made (precision of sensors, temperature control, reactor/bath performance, . . .) that are generally incompatible with industrial applications. Additionally, some commercially available laboratory-scale calorimeters require that the different terms in the energy balance be known *a priori*—in particular, the overall heat-transfer coefficient UA. On the other hand, the tool that we have developed uses a combined hardware and software approach that allows us to estimate the sum of UA and heat losses on-line with no *a priori* knowledge of them by using on-line estimates of the evolution of UA with viscosity and using delayed (on the order of 10 min), but real time, gravimetric conversion to update our estimates of UA and Q_{Loss}.[5–7]

Once information on Q_R is available, it is fed to what can be referred to as a "kinetic"-state estimator that is used to provide information on the evolution of the number of residual moles of monomer as a function of time and a lumped kinetic parameter that is proportional to the product of the total number of particles in the emulsion and the average number of radicals per particle. It was decided to test this adaptive calorimetric + state estimator tool under different conditions. This technique was tested in simulation[6] and with a classical system (i.e., hydrophobic monomers) using both semibatch and periodic shots of a monomer for the copolymerization of styrene (Sty) and butyl acrylate (BuA).[8] However, because these two monomers are relatively hydrophobic, no secondary nucleation can occur during the reaction unless it is expressly provoked. Also, the individual monomer conversions evolve slowly, with no significant exotherms occurring during the course of the reaction. It was judged useful to apply this method to the study of the copolymerization kinetics of methyl methacrylate (MMA) and vinyl acetate (VAc), a copolymerization that is interesting for two major reasons: First, it is very difficult to maintain a constant reactor temperature because the copolymerization is characterized by a large heat release in mid-reaction as we will see below. Second, in systems such as this where the principal monomers are hydrophilic, it can be very difficult to model the evolution of parameters such as N_p and $\bar{n}$, especially in the face of perturbations to normal reactor operation or in the presence of previously undetected impurities and inhibitors. It is therefore interesting to have a tool that allows us to follow such parameters on-line.

Note that the energy balance in eq. (1) uses a single value for the reactor temperature, T_R, and one value of T_j. In the small lab-scale reactor we used in the current work, it is a relatively simple task to define these values. T_j is simply the average of the inlet and outlet temperatures (which differ by only a fraction of a degree), and T_R is measured at a spot halfway between the wall and the impeller. However, in larger, industrial reactors, it is not so simple to measure these quantities. Two solutions can be envisaged: (1) Choose what seems to be the most reasonable temperature (e.g., average of jacket inlet and outlet for T_j) and accept that any error due to this choice will be combined with the estimate of the heat-loss term (that we do not need to know), or (2) change the energy balance approach and use a jacket energy

balance instead of a reactor energy balance to perform the state estimation. In what follows, we will present only the results of the evaluation and examples of how information from this estimator can be applied to the MMA–VAc system. Readers wishing details on the mathematical structure of the estimator are referred to earlier articles.[6,9]

COPOLYMERIZATION KINETICS OF MMA–VAC

Given the fact that both of the monomers to be considered in this work are soluble to different degrees in the continuous aqueous phase, the copolymerization kinetics can be described by the following general model for monomer 1 (generally the more reactive):

$$\frac{dN_1}{dt} = -\mu(t)[M_1^p][k_{p_{12}}\phi_1^p + k_{p_{21}}(1 - \phi_1^p)] - V_w[M_1^w]$$

$$\times \ [R^*]^w[k_{p_{12}}\phi_1^w + k_{p_{21}}(1 - \phi_1^w)] \quad (2)$$

where

$$\mu(t) = \frac{\bar{n}(t)N_p(t)V_e}{N_a} \quad (3)$$

and N_i is the number of moles of monomer i; $[M_i^p]$ and $[M_i^w]$, the concentration of monomer i in the particles and water phase, respectively; ϕ_i^p and ϕ_i^w, the probability of finding a radical ending in a unit of type "i" in the particle and water phases; $[R^*]^w$, the concentration of radicals in the aqueous phase; V_e, the volume of the emulsion (total volume); V_w, the volume of the aqueous phase (water plus dissolved organic components); $\bar{n}$, the average number of radicals per particle; and $N_p(t)$, the number of polymer particles per liter of emulsion. The mole balance for monomer 2 is the same with an appropriate change of subscripts. To model a copolymerization, one needs information on the evolution of the rate constants as a function of time and, perhaps, more importantly, on that of the parameter μ. This second parameter contains both N_p and $\bar{n}$—key parameters which are often difficult to predict. It is for this reason that we choose to estimate μ along with the evolution of the total number of residual moles of both monomers with the adaptive calorimetric approach.

The emulsion homopolymerization of both VAc and of MMA as well as their copolymerization have been studied extensively in the literature. For example, in the case of VAc, a wide range of conditions have been studied that show that $\bar{n}$ depends to a large extent on a number of parameters, including particle size. Several studies looked at the emulsifier-free emulsion polymerization of VAc. For instance, Lange et al.[10] looked at the kinetics of the seeded surfactant-free emulsion polymerization of VAc, using very large seed particles (400 nm) to eliminate water-phase termination. They showed that $\bar{n}$ with such large particles (and in a relatively dilute latex: $N_p \in 10^{13}$–10^{15} particles/liter of water) is on the order of 4–7—a figure much higher than encountered in other works. Other authors[11,12] looked at the relationship between rate and reaction conditions in similar systems. The presence of additives such as TiO_2 in the second study leads to a rate with a dependence on the initiator concentration on the order of 0.86, whereas a different group[11] found a dependence of only 0.6.

Nomura and Harada[13] presented a model that allows one to calculate $\bar{n}$ for VAc (and vinyl chloride) based on an estimate of the radical desorption coefficient. Although this model seems to give reasonable results when compared to experimental results found in the literature, it requires that one know the value of the number of particles per liter of emulsion beforehand (N_p)—not practical from a control standpoint. Nevertheless, they did demonstrate that $\bar{n}$ in a VAc system is governed by radical desorption. Also, the experimental values they cited show that at 50°C $\bar{n}$ can vary from 5×10^{-3} to approximately 0.5 depending on the ratio of the rate of the initiator decomposition to the product of the average number of particles per liter and the desorption coefficient. This model was incorporated into a reactor model for the prediction of polymerization rates, particle diameter, and molecular weight with some success by Penlidis et al.[14] De Bruyn et al.[15] studied the kinetics of the emulsion homopolymerization of VAc and claimed that their γ-radiolysis relaxation studies showed that the exit of radicals from particles on the order of 74 nm in diameter dominates the final value of $\bar{n}$. Their studies showed that at temperatures on the order of 50°C $\bar{n}$ was on the order of 0.07. In a different vein, Kshirsagar and Poehlein[16] looked at the problem of radical entry during VAc polymerization and showed that radical entry into the particles depended on the size of the oligoradicals formed in the aqueous

phase. Kim et al.[17] studied mass transfer in poly-(vinyl acetate) (PVAc) systems and showed that nonionic surfactants produced a higher mass-transfer resistance to monomer entry into the polymer particles than did ionic surfactants.

Cutting and Tabner[18] looked at the emulsion homopolymerization of MMA and later[19] at its core–shell copolymerization with BuA and used ESR to examine radical concentrations in the latex. In the first of these two works, they noted a net increase in the radical concentration per cubic decimeter of reaction mass (and, therefore, of $\bar{n}$ if we assume that no significant coagulation or secondary nucleation took place). In the second study, they found that it was not possible to detect radicals during most of the BuA emulsion homopolymerization phase in the core–shell case, but that during the homopolymerization phase where MMA was at the core of the emulsion particles the radical concentration (and therefore $\bar{n}$) increased as a function of conversion.

Cheong and Kim[20] observed an increase in $\bar{n}$ with conversion in MMA emulsion polymerization. They observed that the average number of radicals per particle increased from well under 1 at low conversions to a value somewhere between just over 2 and 5. The maximum value for $\bar{n}$ seemed to be strongly dependent on the surface charge density of the particles.

Arzamendi and Asua[1] presented a model for the emulsion copolymerization of VAc and methylacrylate (MA) that includes expressions for the estimation of $\bar{n}$. Their results were very promising: The only drawback was that it is necessary to know the termination rate constant for both polymers as well as the cross-termination rate constant. As Othman et al.[21] showed, this can be a difficult exercise even for dilute solution polymerizations. These last authors used a nonlinear estimator to find values of the overall termination rate constant for the solution copolymerization of VAc with BuA and showed that this constant can increase by several orders of magnitude in closed systems in a very short period of time.

Finally, the copolymerization of MMA and VAc was also studied. Dubé and Penlidis[22] looked at the copolymerization of these two monomers in a pilot scale reactor and observed a "stepwise" behavior of the polymerizing system mentioned above. Not surprisingly, they also observed significant composition drift in the copolymer. In the particular case of MMA-*co*-VAc, the difference in the reactivity ratios is such that as soon as the MMA is consumed in a batch reactor the reactor lights off as the VAc begins to polymerize. They also looked at the copolymerization of MMA/VAc in bulk and solution and observed much the same thing.[23]

The copolymerization system considered in this work is thus characterized by a sudden change in the rate of heat release and conversion that should be very difficult to follow. This, coupled with the fact that $\bar{n}$ is a highly complex function of particle size, monomer concentration, and other process parameters means that the reaction is very difficult to model without a certain amount of process-specific information. It is therefore obvious that without extensive work on the kinetics and an excellent model of the gel effect in copolymerization, radical absorption, and desorption (and thus transfer within the particles), it is very difficult indeed to predict values of $\bar{n}$ correctly in systems as complex as VAc/MA, VAc/MMA, or VAc/BuA using typical modeling techniques. For this reason, we decided to use tools such as the "software-sensor" made up of an adaptive calorimeter[24] and nonlinear-state estimators to study what occurs in the reaction under real conditions.[6,9] The goal was to try to obtain good values of $\bar{n}$ at the same time as to provide information on the relative rates of polymerization (or the individual conversions of both monomers) in order to better understand how such parameters vary as a function of reaction conditions. This, in turn, will help us to control the reactor at the production stage.

In what follows, we will use a calorimetric tool to follow both the overall and individual conversion of the monomer on-line. These results, combined with off-line measurements of latex and polymer properties [particle-size distribution (PSD); glass transition temperature (T_g)] allow us to obtain a better understanding of the evolution of the system. Such information will eventually help us to perfect existing mathematical models of this complicated polymerization. The objectives of the current work were therefore twofold: First, to test the response of the adaptive calorimetric technique described in previous works[8,9] for relatively "well-behaved" systems like Sty–BuA, and, second, to show that such a reactor, properly combined with state-estimation techniques and approximate models of the system, can be used to probe the evolution of key, yet difficult to measure, parameters such as the average number of radicals per particle.

Table I   Parameters Used in State Estimator

MMA	$k_p = 2.65 \times 10^6 \exp\left(\dfrac{-5337}{RT}\right)$	Van Herk[25]
	[L mol^{-1} s^{-1}]	
(monomer 1)	$r_1 = 24$	Dubé and Penlidis[22]
VAc	$k_p = 1.49 \times 10^7 \exp\left(\dfrac{-4870}{RT}\right)$	Van Herk[25]
	[L mol^{-1} s^{-1}]	
(monomer 2)	$r_2 = 0.026$	Dubé and Penlidis[22]
ϕ_c (copolymer volume fraction in particles at saturation)	$\phi_c = 0.27$	Gilbert[26]

MODELING AND STATE ESTIMATION

It has been shown[6,21] that calorimetric measurements of the heat of reaction, coupled with occasional gravimetric evaluations of the overall mass conversion, can theoretically be used to follow the rate of reaction (for a more detailed treatment of the calorimetric and state-estimation approach, the reader is directed to these two works). This approach is based on an estimation of the states in the reactor using a model of the polymerization process. Obviously, the better the model, the more representative the estimates of the system states will be. However, it is possible that if one is only interested in following the evolution of monomer conversion and copolymer composition, then polymerization in the water phase can be neglected (see, e.g., Guinot et al.[7]). In this case, eq. (2) simplifies to

$$\frac{dN_i}{dt} = -\mu(t)[M_i^p(t)]\{k_{p_{ij}}\phi_i(t) + k_{p_{ji}}[1 - \phi_i(t)]\} \quad (4)$$

It is true that this simplified model does not take into account everything that happens in the reactor. Chain growth and continuous homogeneous nucleation in the water phase is obviously overlooked. Nevertheless, since estimates of the average number of radicals per particle are based on observed values of the rate of polymerization and aqueous-phase polymerization represents only a small portion of what actually occurs inside the reactor, we believe that the estimates of $\bar{n}$ will contain errors of only a few percent at most if one neglects water-phase polymerization. This is not to say that what goes on in the aqueous phase is unimportant. On the contrary, it is also extremely important to understand how a monomer is partitioned for advanced process control, in order to understand underlying mechanisms such as the formation of oligoradicals and radical entry. The data used in the state estimation are summarized in Table I.

EXPERIMENTAL

Five batch polymerizations with different compositions were considered in the present work (recipes in Table II). All products used in the reactions were obtained from Aldrich (L'Isle d'Abeau Chesnes, France). The monomers VAc and MMA

Table II   Initial Conditions for Homo- and Copolymerization Experiments

HP–MMA	MMA	600 g	CP30-70	MMA	180 g
	SDSS	3.0 g		VAc	420 g
				AOT-75	4.0 g
HP–VAc	VAc	600 g	CP50-50	MMA	300 g
	SDSS	3.0 g		VAc	300 g
				AOT-75	4.0 g
All experiments			CP70-30	MMA	420 g
NaHCO$_3$: 1.84 g, KPS: 1.84 g,				VAc	180 g
water: 2400 g				AOT-75	4.0 g

were purified by distillation before use. The free-radical initiator potassium persulfate (KPS) was used as received. Either pure sodium dioctyl sulfosuccinate (SDSS) or AOT-75 (SDSS 75% in water 25%) was used as the surfactant in all experiments (i.e., 3 g of SDSS contains the same amount of surfactant as 4 g of AOT-75).

Polymerizations were carried out in a 7-L, jacketed glass reactor with an external cooling jacket. The cooling fluid is water, which is fed to the jacket at a constant rate at a constant temperature. Note that no attempt is made to maintain an isothermal operation in the reactor. At the beginning of each reaction, the reactor is filled with the water, surfactant, buffer, and monomer. It is then heated to the desired temperature before adding the initiator in a small quantity of water.

Gravimetric samples were obtained on-line and overall conversion was evaluated by drying a known quantity of latex on an infrared balance. This information is available at a frequency of one data point every 10–15 min. Verification of individual conversions was obtained off-line from proton NMR spectra or by using a residual chromatographic technique. Glass transition temperatures were estimated from dynamic scanning calorimetry (DSC) thermograms. The DSC thermograms were obtained by using a TA Instrument MDSC 2920 calibrated with high-purity indium. For the needs of this study, we worked at a temperature range of -150 to $150°C$ at a constant heating rate of 10 or 20 K min^{-1}. Liquid nitrogen was used to cool the sample and as the reference for the desired temperature, and a constant argon flow was purged into the reactor cell.

Average particle sizes were obtained for different samples using dynamic light scattering, and a field flow fractionation (FFF) device was used to obtain a particle size distribution for the MMA homopolymers. Molecular weights were measured by size-exclusion chromatography on a Waters 510 gel permeation chromatograph equipped with a 1.2-m-long PSS gel mixed category B column. The eluant used was THF at a flow rate of 1.2 mL/min, and the sample volume was 20 μL in a 1% (w/w) solution. The apparatus was calibrated with PMMA.

RESULTS

Validation of On-line Estimation Techniques

As stated above, one of the principal motivations of the current work was to validate the state

estimation and calorimetric approach for highly exothermic, rapidly evolving reactions. In principle, this rapidly evolving, two-step behavior should be difficult to follow on-line. However, it can be seen from the results in Figures 1–3 that the adaptive calorimetric-state estimator and kinetic estimator function very well. The adaptive calorimetric technique previously discussed was applied directly to the three copolymerizations discussed here, and the overall conversion curves shown in Figures 1(a)–3(a) were obtained on-line in real time. The heat balance parameters (and, in particular, UA) were continually updated using on-line gravimetric data. The values of Q_R were then fed to the kinetic-state estimator to obtain estimates of the evolution of the number of moles of MMA and VAc remaining in the reactor as well as of μ. Note that the experimental values of the individual conversions of VAc are usually slightly lower than the estimated values at the beginning of the experiment because they are calculated from the measured gravimetric conversion plus the conversion of MMA measured by GC. They are, therefore, quite sensitive to small errors at low conversions, but it should be noted that once the conversion of VAc reaches significant levels these small errors disappear.

For the sake of comparison, the homopolymerization of VAc and of MMA was also carried out in the calorimeter. The results of the estimation are shown in Figures 4 and 5. Note that in the experiments HP–VAc and HP–MMA the estimation of Q_R was done off-line. Nevertheless, the technique applied is identical, and the results obtained are coherent with those found for the copolymerization experiments. Note also that the estimation of Q_R was stopped almost immediately in the case of VAc (Fig. 5) once the conversion reached 100%—this explains the rather abrupt drop in Q_R. One would expect the value to drop off a bit more slowly if the estimation were continued longer.

Note that the temperature profiles shown in Figures 1–5 are the outputs of the calorimetric-state estimator. However, it is important to point out that they are essentially identical to the measured values, which are not shown here for this reason.

The success of the techniques tested here in estimating the real value of the conversion on-line is due to the adaptive nature of the approach, which allows us to obtain precise estimates of $UA(T_R - T_j) + Q_{Loss}$ as it evolves in the reactor. Contrary to the case in a large number of the previously cited works, this technique allows one
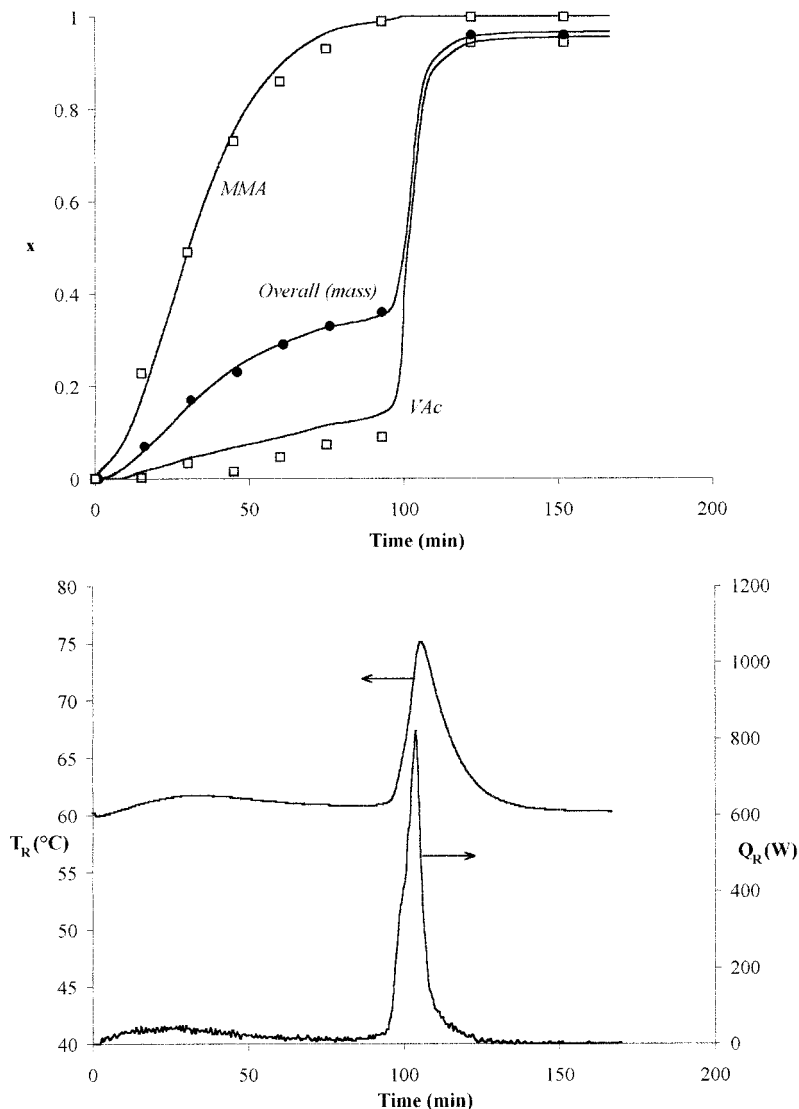
Figure 1   Results of the kinetic study for the copolymerization CP 30-70 and estimation of reactor temperature and heat generation rate due to the reaction.

to perform an energy balance regardless of what is happening in the reactor (short of total flocculation, of course). This tool, combined with the nonlinear kinetic estimator, gives us very reasonable estimates of the evolution of the monomer composition and heats of reaction as a function of time.

In Figures 1–3, we can clearly see the "2-step" nature of the polymerization reaction. In the early stages of polymerization, the MMA, which has a reactivity ratio approximately 925 times higher than that of VAc, polymerizes first due to the fact that almost all of the radicals in this system are terminated by MMA units and that the few VAc radicals that exist are also very re-

active—but, particularly, toward MMA. If we use values of 24 for r_{MMA} and 0.026 for r_{VAc}, it is very easy to show that for values of f_1 greater than 0.01 (i.e., conversion of MMA less than 99%), the value of ϕ_{MMA} is greater than 0.99 (i.e., a situation very close to the homopolymerization of MMA). Once the MMA has been totally consumed, the VAc is free to "homopolymerize." Since it polymerizes very rapidly with respect to the MMA (according to the data compiled by van Herk,[25] the k_p of VAc is on the order of 9460 L mol^{-1} s^{-1} at 60°C versus 833 for MMA at the same temperature), the reaction lights off very quickly. This, combined with a higher enthalpy of polymerization for VAc (-88 kJ/mol versus. -56
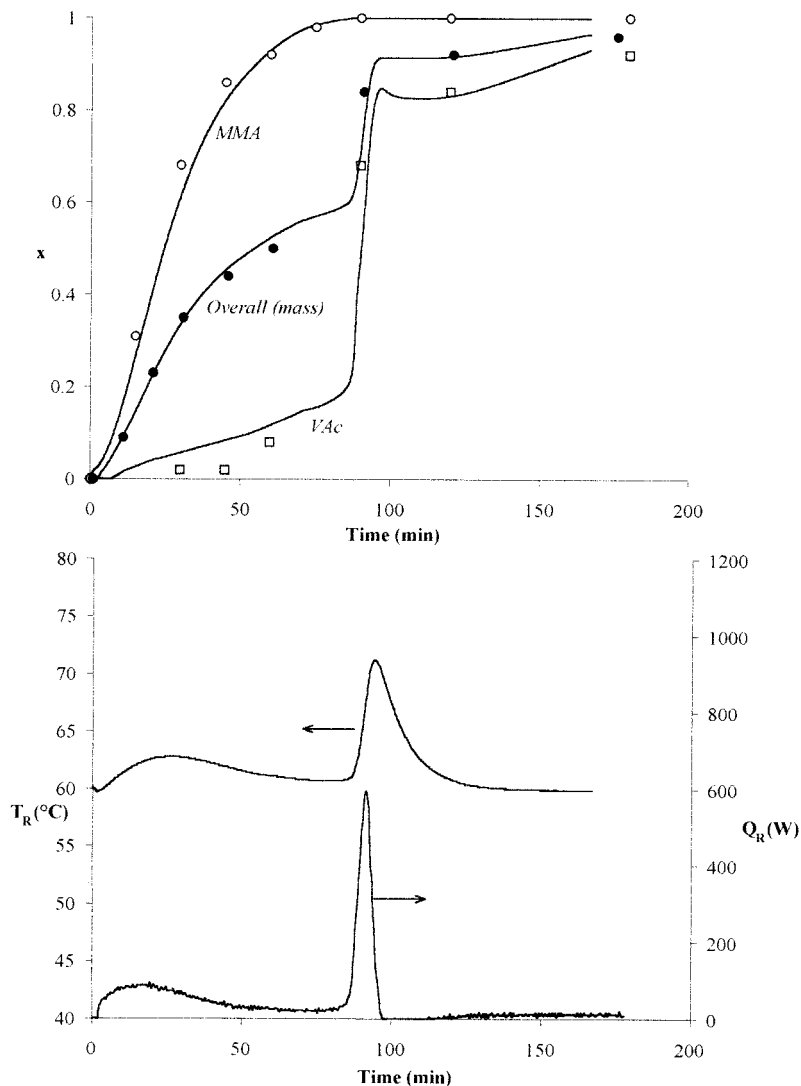
Figure 2 Results of the kinetic study for the copolymerization CP 50-50 and estimation of reactor temperature and heat generation rate due to the reaction.

kJ/mol for MMA), leads to a significant peak in the value of Q_R in all the experiments. This generalized behavior can be seen for all three ratios of monomer composition studied here.

Note that in the experiments presented in Figures 1–5 the reason for these temperature increases is obviously the fact that the reactions are highly exothermic, but also that the reactor cooling jacket has a fixed inlet temperature. No attempt was made to maintain an isothermal operation in the reactor to demonstrate that the adaptive calorimetric technique can provide accurate process information under nonisothermal conditions.

It is important to note that the estimation technique seems to predict negative values of the heat generated by reaction in experiments CP 50-50 and CP 70-30 just after the large peak in the rate of heat generation. Given its relatively low boiling point (72°C for pure VAc, higher in solution with polymer), it is possible that a fair amount of VAc is evaporated during the portion of the curve where we see a rapid temperature increase and is then cooled and liquefied in the condenser. The reaction rates are always very low (seen from the conversion–time curves) at these points which occur just after a large heat release in the reaction. Since this addition of the cold monomer from the condenser is not taken into account in the energy balance, it is highly possible that when Q_R is, in reality, very low then the estimator might provide a negative energy generation rate. This is similar
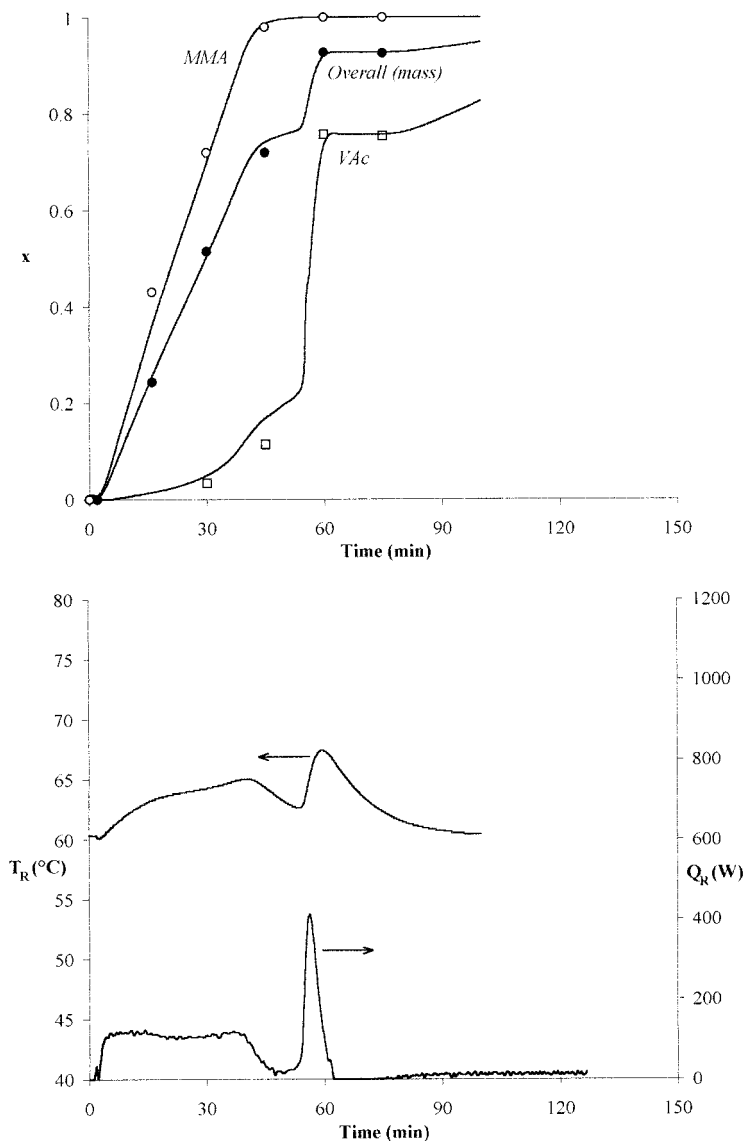
Figure 3 Results of the kinetic study for the copolymerization CP 70-30 and estimation of reactor temperature and heat generation rate due to the reaction.

to the very short periods of "cooling" right at the beginning of the reaction where we inject the initiator dissolved in a small amount of water at ambient temperature. All the copolymerizations show this behavior, which quickly vanishes.

The value of μ obtained from the on-line data is shown in Figure 6 for the three copolymerizations. These curves will be analyzed in more detail in the following subsection, but it should be evident that, at least for CP 30-70 and CP 50-50, the sudden changes in the conversion–time and Q_R–time curves are not due to particle renucleation. If they were, then μ should increase dra-

matically and by a factor equal to the increase in Q_R (e.g., by a factor of around 75 for CP 30-70) at the light-off point. As can be seen from Figure 6, this is definitely not the case—if anything, μ decreases at the light-off point (which is normal). Thus, even without having detailed information about the separate values of N_p and $\bar{n}$ for the different experiments, μ provides valuable information about the behavior of the reactor in real time.

It is also interesting to note from Figures 1–5 that only those experiments where the initial charge was very rich in MMA (CP 70-30, HP–
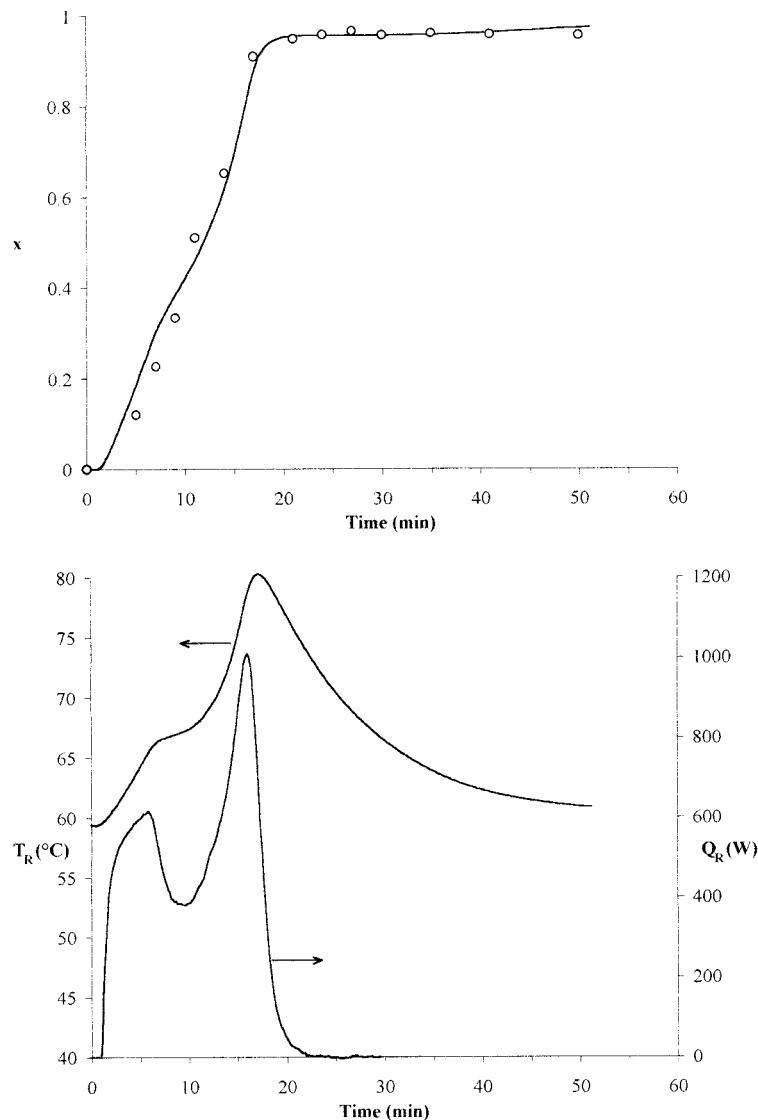
Figure 4   Results of the kinetic study for HP–VAc and estimation of reactor temperature and heat generation rate due to the reaction.

MMA) show a clear "stage II"-type kinetics. This stage lasts for approximately 25 min for HP–MMA and about half again as long in the case of CP 70-30. These two experiments both show values of μ that are relatively constant during these time periods, suggesting that both $\bar{n}$ and N_p remain stable.

As discussed in numerous other works, this type of information (overall and individual conversions versus. time, and μ) is, of course, indispensable for the proper monitoring and control of emulsion polymerization processes. Rapidly available information on the evolution of monomer composition allows one to understand how copolymer composition is evolving and provides accurate data for updating model-based estimates of the molecular weight distribution, glass transition temperature, etc. However, this is not the only motivation behind using on-line information from adaptive calorimetry combined with nonlinear state estimators. In effect, this is also an excellent method for obtaining accurate and continuous process information that can be combined with information obtained off-line (e.g., particle size and T_g) in order to obtain a better understanding of the physical processes occurring during the polymerization.
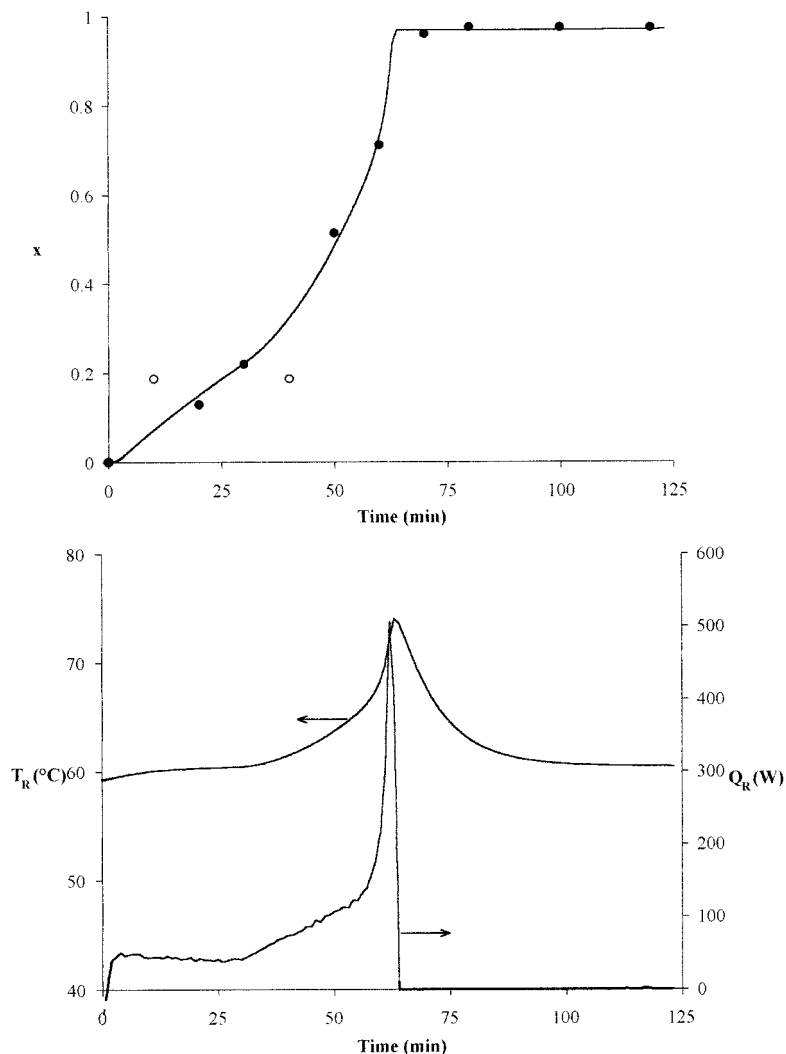
Figure 5 Results of the kinetic study for HP–MMA and estimation of reactor temperature and heat generation rate due to the reaction. Open points in conversion–time graph assumed to be erroneous measurements.

Off-line Interpretation of Experimental Data: An Analysis of the Copolymerization System

The relationship between the two-step nature of the batch copolymerizations and the glass transition temperature of the final polymer can clearly be seen from Table III. The T_g of PMMA was found to be on the order of 114–119°C depending on the product examined. The value for PVAc was a bit less clear, ranging over an interval of 27–37°C (Lesko and Sperry[27] gave a value of 29°C for the PVAc homopolymer). These homopolymer values seem reasonable and can explain the results observed for the evolution of the T_g of the copolymers. It can be seen from Figures 1(a)–3(a) that, during the early stages of polymerization, the co-

polymer is going to be composed of a majority of MMA and that the relatively high values of T_g correspond almost to that of an MMA homopolymer. However, at the end of the polymerization, two peaks corresponding to two different T_g's are seen on the thermograms—one corresponding to a copolymer very rich in VAc, and the other, to a copolymer rich in MMA.

To understand more about the underlying mechanisms of polymerization, and, in particular, to estimate values for $\bar{n}$ and how particles are nucleated in this system, one needs to have other information about the process. It should be clear from eqs. (2 and 3) that if one has a value for $N_p V_e$ it is a relatively easy task to deduct values of $\bar{n}$
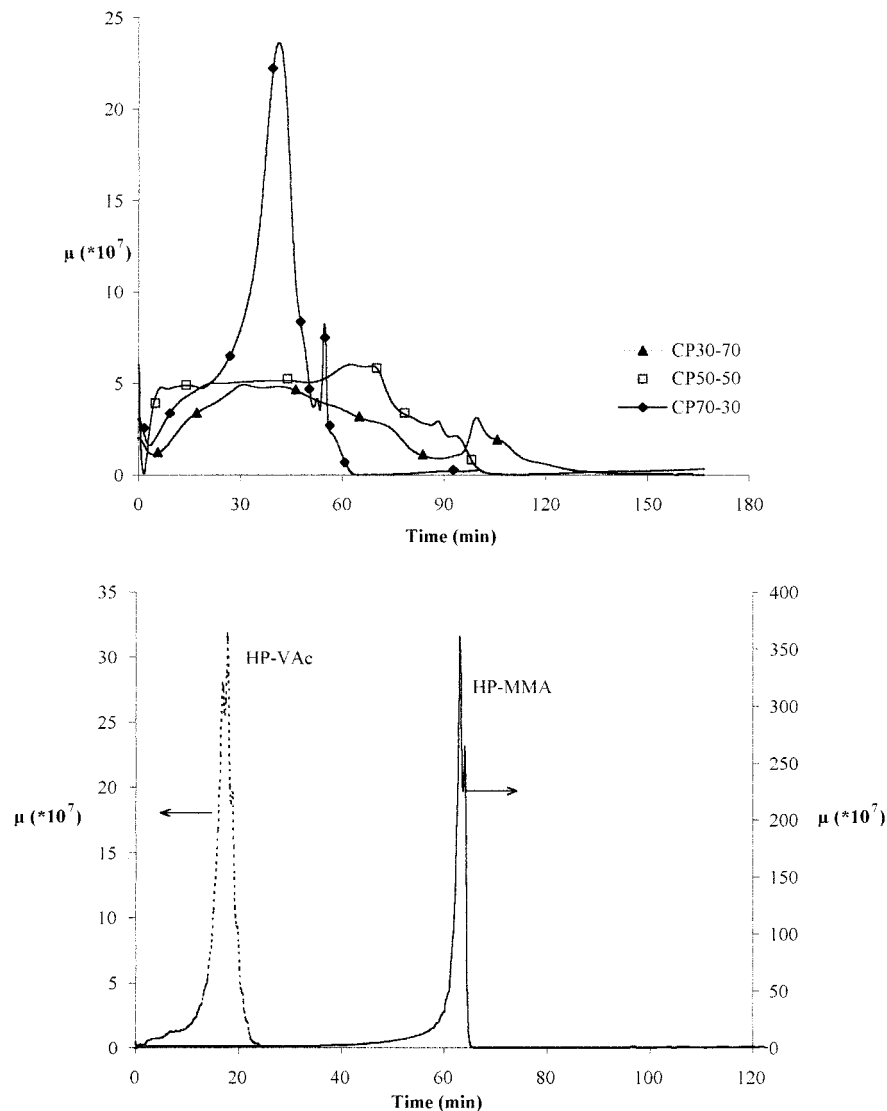
Figure 6 Dimensionless parameter μ as a function of time for the three copolymerizations.

Table III   Evolution of T_g

CP 30-70		CP 70-30		CP 50-50	
xg	T_g (°C)	xg	T_g (°C)	xg	T_g (°C)
0.07	113	0.24	106	0.09	117
0.23	108	0.51	118	0.44	118
0.36	95	0.72	110	0.50	107
0.96	45 and 97	0.93	38 and 113	0.92	37 and 103

HP–MMA: final T_g = 119°C (114°C for sample of Lucryl®—commercial PMMA from BASF, Ludwigshafen, Germany). HP–VAc: Final $T_g \in$ 27–37°C.

from the on-line estimation of the parameter μ. To evaluate $\bar{n}$ for this system and to try to probe the mechanisms underlying particle nucleation in this copolymerization system, particle-size measurements were performed throughout the course of all experiments. In addition, an MMA homopolymerization was also run under similar conditions (HP–MMA). The average number of particles and average particle sizes are shown in Figure 7.

It is interesting to note for the homopolymerizations that although the final particle size is similar for both PVAc and PMMA latices the kinetics of particle growth are not at all the same.
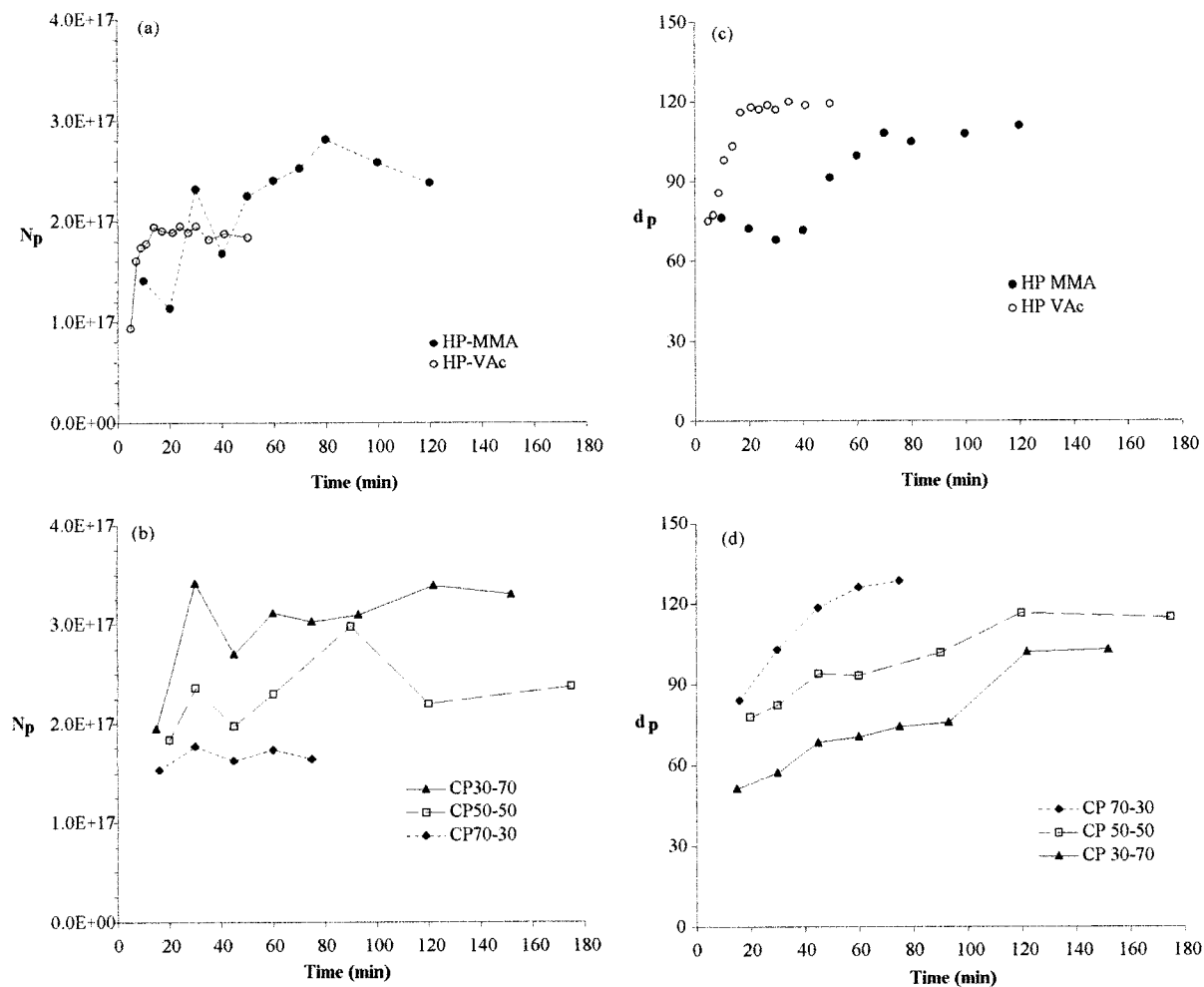
Figure 7 Evolution of N_p as a function of time (a) for the two homopolymerization systems and (b) for the copolymerizations. Note that N_p is based on average particle sizes measured by light scattering: (c) homopolymerization; (d) copolymerization.

As one would expect, and as can be seen in Figures 4 and 5, the rate of polymerization of VAc is much higher than that of MMA. The VAc reaction is finished in 20 min and the number of particles per liter of emulsion seems to increase for approximately 15 min and remains stable for the last few minutes of the reaction. The same can be said for MMA polymerization, where particles seem to be formed during most of the reaction as well. Since it is well known that particle formation can occur by both micellar and homogeneous routes for both of these (relatively) hydrophilic monomers, this result is not surprising. A more detailed discussion of particle nucleation will appear in a forthcoming article.

The evolution of $\bar{n}$ as a function of time can be seen from Figure 8. These values were calculated

from the values of μ known values of V_e and from the measured values of N_p. For the copolymerization experiments, N_p was set at 3.2×10^{17} particles/liter emulsion for CP 30-70, 2.32×10^{17} particles/liter emulsion for CP 50-50, and 1.62×10^{17} particles/liter emulsion for CP 70-30. Although it is possible that there is a slight evolution of N_p during the initial instants of the copolymerization experiments such as there is for the homopolymers, it seems reasonable to use a single, average value given the limited number of points and the rather large imprecision associated with the use of the QELS technique employed here. For the homopolymers, N_p was calculated using values interpolated from the points in Figure 7 since no average value could be discerned. Note that it is evident that the values of $\bar{n}$ thus calculated for
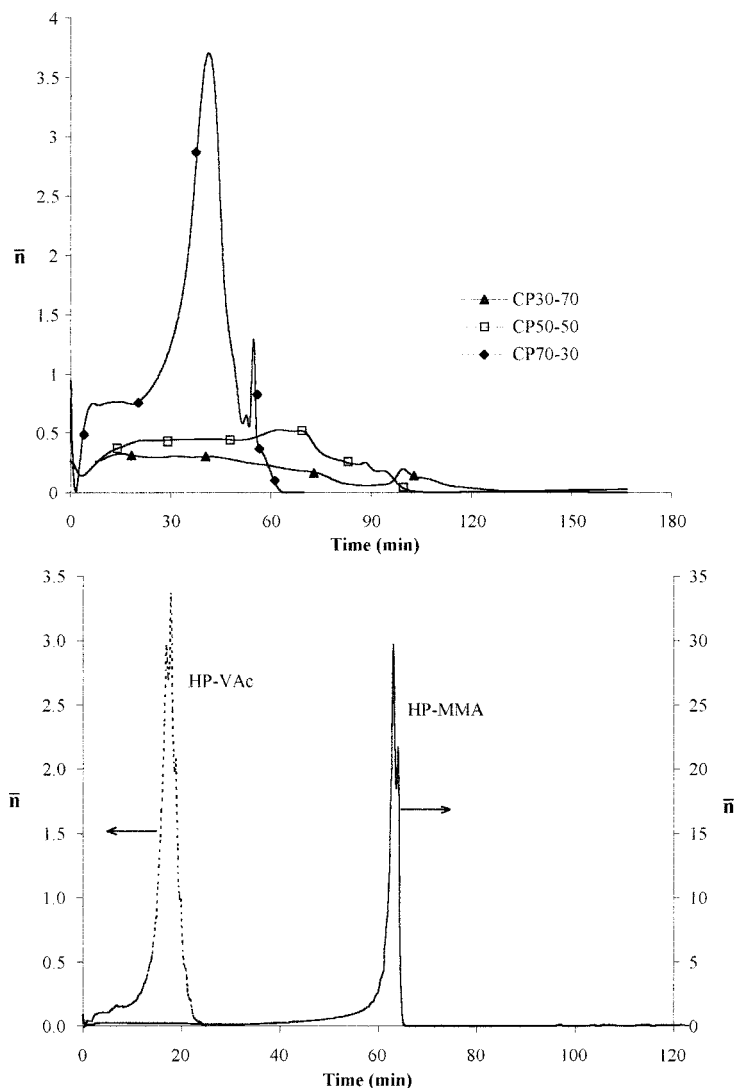
Figure 8 Evolution of $\bar{n}$ for (a) the three different copolymerizations and (b) the homopolymers.

the copolymerization system are not valid for the first few minutes of the reactions during the nucleation stage. Also, very small errors are contained in $\bar{n}$ since we neglected water-phase polymerization, but, as stated above, these errors are very small (likely to be less than 1%) compared to the uncertainties in the values of the rate constants and reactivity ratios found in the literature.

As one would expect, the value of $\bar{n}$ for the homopolymerization of MMA is rather high. It increases from an initial value of 0.3 at the early stages of reaction to over 30 just before the limiting conversion is established. These results are in good agreement with those of

Cheong and Kim.[20] In the case of VAc, the results are also within the range reported in the literature. At the onset of polymerization, when the particles are relatively small (on the order of 75 nm in diameter), $\bar{n}$ is on the order of 0.1. As the particles grow, its value increases to a maximum of just over 3. These results are not unexpected, as the trends (i.e., $\bar{n}$ increasing as polymer concentration in the particles increases and as the size of the particles increases) are what one expects to find based on a review of the literature. However, it should be clear that given the sensitivity of a quantity such as $\bar{n}$ to a number of process variables a tool such as this one is very useful in trying to model it.

If one considers the evolution of $\bar{n}$ in the case of the copolymerizations, it is not unexpected to find higher values in the experiments containing larger quantities of MMA. For example, the highest value of $\bar{n}$ in a copolymerization experiment is found from experiment CP 70-30. However, its maximum is almost an order of magnitude smaller that that observed for HP–MMA. It is clear that adding VAc to the reaction mixture leads to consistently lower values of $\bar{n}$—the exact value found depending on the rate of disappearance of MMA in the system as well as on the quantity of VAc. As pointed out in the Introduction, this is to be expected given the high rates of radical desorption associated with VAc—and the fact that $\bar{n}$ for PVAc is well over one order (or even two) smaller than that of PMMA.

It is interesting to note that although the homopolymerization of MMA is significantly slower than that of VAc, the copolymerization reaction proceeds more rapidly as the MMA content is increased. Furthermore, the point at which the MMA is almost totally consumed occurs earlier and earlier. In fact, we reach an MMA conversion of 99% (close to the point where the reaction begins to accelerate very rapidly) at 93.3, 78.2, and 46.1 min for the copolymerizations containing 30, 50, and 70% MMA (w/w), respectively. The reason for this can be seen from Figure 8, where $\bar{n}$ is inversely proportional to the amount of VAc in the system. For the copolymerizations CP 30-70 and CP 50-50, the changeover from a system rich in MMA radicals (arbitrarily chosen at $x_{MMA} = 99\%$) to one rich in VAc occurs at overall mass conversions of 35 and 58%, respectively. In these two cases, there is not enough polymer in the particles to induce a strong Tromsdorff effect and $\bar{n}$ remains relatively low. CP 30-70 obviously contains more VAc than the other experiment, and the overall value of $\bar{n}$ remains consistently lower, as one would suspect.

On the other hand, in the case of CP 70-30, the gel effect becomes important before the critical point, and, therefore, $\bar{n}$ increases quite early in the reaction, reaching a maximum value of 3.7 at 41.2 min. This value is over seven times higher than the maximum of 0.5 seen for CP 50-50 and over 12 times the maximum of 0.31 seen for CP 30-70. In addition to the gel effect, there is also the fact that the particles contain less VAc, and, therefore, $\bar{n}$ is higher for this experiment in the early stages of reaction, before the gel effect sets in. These results are also consistent with the observations of Cutting and Tabner[18] who noted an
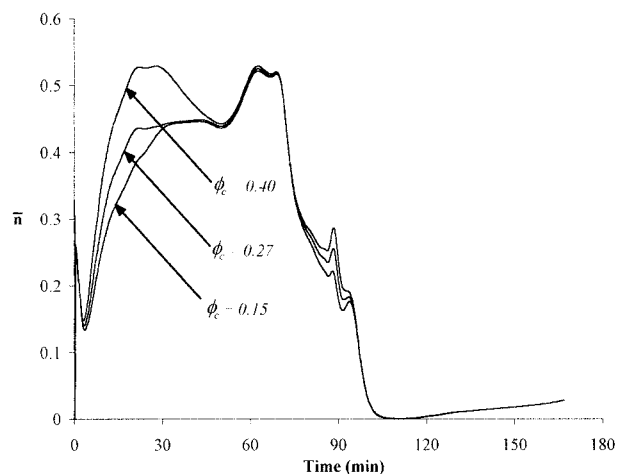

Figure 9 Sensitivity of $\bar{n}$ to variations in the solubility of polymer in the growing particles (ϕ_c = volume fraction of polymer at saturation) for the experiment CP 50-50. $\phi_c = 0.27$ for the base case.

increase in the number of radicals during the polymerization of MMA.

Finally, the sensitivity of $\bar{n}$ to changes in the volume fraction of the polymer at saturation (ϕ_c) is shown in Figure 9. It is clear that although this parameter is important the results presented in the current article are not particularly sensitive to changes in ϕ_c. Although the results are only shown for CP 50-50, the trend is identical for the other experiments discussed in the current work. Increasing ϕ_c by 50% leads to a slightly higher prediction for $\bar{n}$ since this corresponds to a lower concentration of monomer in the particle. Because the estimation of μ is based on an evaluation of the rate of polymerization, the only way that one can compensate for a decrease in monomer concentration is to increase the value of $\bar{n}$.

The information on $\bar{n}$ can also be used to help us understand why the molecular weight distribution (MWD) varies as it does. The values obtained for the two homopolymers and for experiments CP 70-30 and CP 50-50 are shown in Figure 10. The molecular weights for experiment CP 30-70 were too high to dissolve in THF and it was therefore not possible for us to measure them. This is, in fact, consistent with the findings shown here. Although the PVAc homopolymer has a significantly lower molecular weight (and slightly wider MWD) than that of the PMMA homopolymer, it was found that the more VAc there was in the copolymer mixture the higher the average molecular weight of the copolymer. It is possible that this is due to the decrease in the value of $\bar{n}$ as the VAc content of the initial charge is
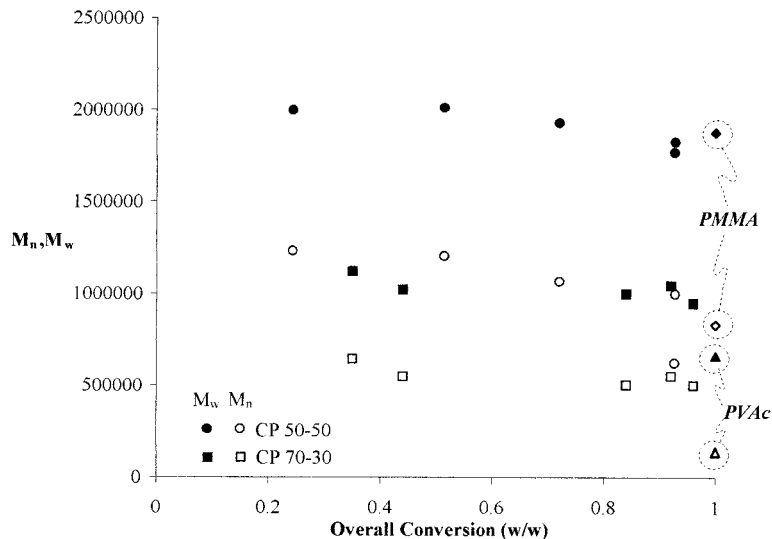
Figure 10 Evolution of number- and weight-average molecular weights (M_n, M_w) for CP 50-50 and CP 70-30 as a function of overall conversion compared to final values for the two homopolymers. (Open symbols) M_n; (closed symbols) M_w. Mark–Houwink parameters for MMA: $K = 9.44 \times 10^{-5}$ dL/g, $a = 0.719$ (Hutchinson et al.[28]); for VAc: $K = 22.4E - 5$ dL/g, $a = 0.674$ (Hutchinson et al.[29]).

increased. Regardless of the amount of VAc in the initial charge, most of the radicals in the polymer particles terminate in an MMA group and thus the polymerization is, as we said above, similar to an MMA homopolymerization, and, thus, we expect to have relatively high molecular weights. However, the more VAc is in the initial charge, the lower the value of $\bar{n}$ (probably due to high rates of desorption of the few radicals that actually terminate in a VAc group) and, thus, the higher the value of M_w since termination of the growing radicals decreases. Hence, the copolymer 70-30 has the molecular weights closest to those of the PMMA homopolymer, and as we increase the ratio of VAc : MMA, the molecular weight increases. Note that we do not want to give the impression that this is the only reason. Increased branching due to high rates of transfer to the polymer in the presence of VAc will also contribute to this observation.

It should be noted that these MWD data are essentially only useful for comparison between the experiments shown here. The MWD calibration only increases to 5,000,000 for the machine available in our laboratories, and, thus, we can only extrapolate to find the high MW tail of the distribution curve. Thus, the average values presented here for CP 50-50 and CP 70-30 might be slightly underestimated. Second, no correction was applied to the data for the copolymerizations. At low conversions, where the polymer is essen-

tially composed of large fractions of MMA, this is probably acceptable. Although this simplification seems acceptable at higher conversions, where a significant fraction of VAc begins to be incorporated into the polymer, strictly speaking, it is not acceptable to report uncorrected data.

CONCLUSIONS

We have demonstrated that the combination of adaptive calorimetry and on-line state estimation proposed in earlier articles[6–8] for emulsion polymerization yields accurate values of the evolution of the overall and individual conversions, as well as of a lumped kinetic parameter even in rapidly evolving, complex emulsion polymerizations. The robustness of this technique can be seen not only by the excellent agreement between predicted values of the individual monomer conversion, but also that this technique can be used in highly nonisothermal reactions, with a very sudden, significant energy release [Figs. 1(b)–3(b)]. We can thus conclude that the adaptive calorimetric technique can be used safely and under a wide range of difficult and industrially relevant conditions in order to predict the evolution of the individual monomer composition in emulsion copolymerization systems.

Furthermore, the calorimetric data coupled with the state estimator provided very useful information for the evaluation of difficult to measure quantities such as $\bar{n}$ and can help to explain observations in the evolution of the molecular weight distribution and the evolution of the glass transition temperature of the copolymers.

REFERENCES

1. Azarmendi, G.; Asua, J. M. Ind Eng Chem Res 1991, 30, 1342.
2. Saenz de Buruaga, I.; Arotçarena, M.; Armitage, P. D.; Gugliota, L. M.; Leiza, J. R.; Asua, J. M. Chem Eng Sci 1996, 51, 2781.
3. Moritz, H. U. In 3rd International Workshop on Polymer Engineering; Reichert, K. H.; Geisler, U., Eds.; VCH Verlag: Berlin, 1989.
4. Varela De La Rosa, L.; Sudol, E. D.; El-Aasser, M. S.; Klein, A. J Polym Sci Part A Polym Chem 1996, 34, 461.
5. McKenna, T. F.; Févotte, G.; Graillat, C.; Guillot, J. Trans I ChemE A 1996, 74, 340.
6. Févotte, G.; Hammouri, H.; McKenna, T.; Othman, S. Chem Eng Sci 1998, 53, 773.
7. Guinot, P. A.; Othman, N.; Févotte, G.; McKenna, T. Polym React Eng, to appear.
8. Othman, N.; Santos, A. M.; Févotte, G.; McKenna, T. F. Macromol Chem; Macromol Symp, to appear.
9. McKenna, T. F.; Othman, S.; Févotte, G.; Santos, A. M.; Hammouri, H. Polym React Eng, to appear.
10. Lange, D. M.; Poehlein, G. W.; Hayashi, S.; Komatsu, A.; Hirai, T. J Polym Sci Part A Polym Chem 1991, 29, 785.
11. Brooks, B. W.; Wang, J. Polymer 1993, 34, 119.
12. Moustafa, A. B.; Abd El Hakim, A. A.; Mohamed, G. A. J Appl Polym Sci 1997, 63, 239.
13. Nomura, M.; Harada, M. J Appl Polym Sci 1981, 26, 17.
14. Penlidis, A. E.; MacGregor, J. F.; Hamielec, A. E. Polym Process Eng 1985, 3, 185.
15. De Bruyn, H.; Gilbert, R. G.; Ballard, M. J. Macromolecules 1996, 29, 8666.
16. Kshirsagar, R. S.; Poehlein, G. W. J Appl Polym Sci 1994, 54, 909.
17. Kim, J. I.; Vanderhoff, J. W.; Klein, A. J Appl Polym Sci 1995, 58, 279.
18. Cutting, G. R.; Tabner, B. J. Macromolecules 1993, 26, 951.
19. Cutting, G. R.; Tabner, B. J. Eur Polym J 1997, 33, 213.
20. Cheong, I.-W.; Kim, J.-H. Colloid Polym Sci 1997, 275, 736.
21. Othman, S.; Barudio, I.; Févotte, G.; McKenna, T. Polym React Eng 1999, 7, 1.
22. Dubé, M. A.; Penlidis, A. Polym Int 1995, 37, 235.
23. Dubé, M. A.; Penlidis, A. Polymer 1995, 36, 587.
24. Févotte, G.; Barudio, I.; Guillot, J. Thermochim Acta 1996, 289, 223.
25. van Herk, A. M. JMS-Rev Macromol Chem Phys C 1997, 37, 633.
26. Gilbert, R. G. Emulsion Polymerization: A Mechanistic Approach; Academic, Harcourt and Brace: London, 1995.
27. Lesko, P. M.; Sperry, P. R. In Emulsion Polymerization and Emulsion Polymers; Lovell, P. A.; El-Aaseer, M. S., Eds.; Wiley: West Sussex, 1997; Chapter 13.
28. Hutchinson, R. A.; McMinn, J. H.; Paquet, D. A., Jr.; Beuermann, S.; Jackson, C. Ind Eng Chem Res 1997, 36, 1103.
29. Hutchinson, R. A.; Paquet, D. A., Jr.; McMinn, J. H.; Beuermann, S.; Fuller, R. E.; Jackson, C. DECHEMA Monograph 1995, 131, 467.